

1 Satellite-derived Ecosystem Functional Types capture ecosystem 2 functional heterogeneity at regional scale

3 Beatriz P. Cazorla^{1,2*}, Ana Meijide³, Javier Cabello^{1,4}, Julio Peñas^{1,5}, Rodrigo Vargas⁶, Javier Martínez-
4 López^{1,2,7}, Leonardo Montagnani⁸, Alexander Knohl⁹, Lukas Siebicke⁹, Benimiano Gioli¹⁰, Jiří Dušek¹¹,
5 Ladislav Šigut¹¹, Andreas Ibrom¹², Georg Wohlfahrt¹³, Eugénie Paul-Limoges¹⁴, Kathrin Fuchs¹⁵,
6 Antonio Manco¹⁶, Marian Pavelka¹¹, Lutz Merbold¹⁷, Lukas Hörtnag¹⁸, Pierpaolo Duce¹⁰, Ignacio
7 Goded¹⁹, Kim Pilegaard¹², Domingo Alcaraz-Segura^{1,2,4}

8
9 ¹Andalusian Center for Global Change – Hermelindo Castro (ENGLIBA), University of Almería, 04120 Almería, Spain.

10 ²Interuniversity Institute of Earth System Research in Andalusia (IISTA), 18006 Granada, Spain.

11 ³Environment Modeling, Institute of Crop Science and Resource Conservation, University of Bonn, Niebuhrstraße 1a, 53113
12 Bonn, Germany.

13 ⁴Department of Biology and Geology, University of Almería, 04120 Almería, Spain.

14 ⁵Department of Botany, University of Granada, 18006 Granada, Spain.

15 ⁶[School of Life Sciences, Arizona State University, Tempe, AZ, USA](#)<sup>Department of Plant and Soil Sciences, University of
16 Delaware, Newark, Delaware, USA.</sup>

17 ⁷Department of Ecology, University of Granada, 18006 Granada, Spain.

18 ⁸Faculty of Agricultural, Environmental and Food Sciences, Free University of Bolzano, Italy.

19 ⁹University of Goettingen, Bioclimatology, Büsgenweg 2, 37077 Göttingen, Germany.

20 ¹⁰CNR – IBE, Institute of Bioeconomy, Firenze, Italy.

21 ¹¹Department of Matters and Energy Fluxes, Global Change Research Institute CAS, Brno, Czech Republic.

22 ¹²Department of Resource and Environmental Engineering, Technical University of Denmark, Kongens Lyngby, Denmark.

23 ¹³Department of Ecology, University of Innsbruck, Innsbruck, Austria.

24 ¹⁴Department of Geography, University of Zurich, Switzerland.

25 ¹⁵Karlsruhe Institute of Technology, Institute of Meteorology and Climate Research - Atmospheric Environmental Research,
26 Garmisch-Partenkirchen, Germany.

27 ¹⁶Institute for Agriculture and Forestry Systems in the Mediterranean (ISAFoM), National Research Council of Italy, P.le E.
28 Fermi 1-Loc, Porto del Granatello 1, 80055 Portici, Italy.

29 ¹⁷Department of Agroecology and Environment, Reckenholzstrasse 191, 8046 Zurich, Switzerland.

30 ¹⁸Department of Environmental System Science, Institute of Agricultural Science, Zurich, Switzerland.

31 ¹⁹European Commission, Joint Research Centre, Ispra, Italy.

32 *Correspondence to:* Beatriz P. Cazorla (b.cazorla@ugr.es)

33 **Abstract.** Assessing ecosystem functioning is crucial for managing and conserving ecosystems and their services. Numerous
34 ways to evaluate ecosystem functioning have been developed, using species traits, such as Plant Functional Types (PFTs), flux
35 measurements with [the](#) Eddy Covariance (EC) technique, and remote sensing techniques. We propose that the spatial
36 heterogeneity in ecosystem functioning at a regional scale can be assessed and monitored using satellite-derived Ecosystem
37 Functional Types (EFTs): groups of ecosystems or patches of the land surface that share similar dynamics of matter and energy
38 exchanges. We hypothesize that, as observed for PFTs, different EFTs should have distinct patterns and magnitudes of Net
39 Ecosystem Exchange (NEE) of carbon dioxide measured using the EC technique. We derived EFTs [from based-on-the](#) 2001-
40 2014 time-series of satellite images of the Enhanced Vegetation Index (EVI) and compared them with NEE measurements

Con formato: Sin Superíndice / Subíndice

(derived from in situ field observations using the EC technique) across 50 European sites. Our results show that distinct EFTs classes display significantly different dynamics and magnitudes of NEE and that EFTs perform marginally better than PFTs in explaining NEE regional patterns. Land-cover maps based on PFTs are difficult to update on an annual basis and are not sensitive to changes in ecosystem performance (e.g., droughts or pests) that do involve short-term changes in PFT composition. In contrast, satellite-derived EFTs are sensitive to short-term changes in ecosystem performance. Satellite-derived EFTs are an ecosystem functional classification built from satellite observations that allow the identification of homogeneous land patches ~~based on~~ ~~in terms of~~ ecosystem functions, e.g., ecosystem net productivity measured on the ground as NEE. Satellite-derived EFTs can be recalculated annually, providing a straightforward way to assess and monitor interannual changes in ecosystem functioning and functional diversity. [essential matter for biodiversity and carbon management programs.](#)

1 Introduction

Ecosystem functioning and functional diversity are critical issues ~~in~~ ~~of~~ current ecological research (Jax, 2010; Violle et al. 2014, 2017; Tilman et al. 2014; Pettorelli et al. 2018; Villarreal et al. 2018; Malaterre et al. 2019; Díaz et al. 2020). Quantifying, monitoring, and understanding ecosystem functioning help provide insights into the management and conservation of ecosystems and their services (Cabello et al. 2012; Pettorelli et al. 2018; Nicholson et al. 2021). Variables capable of describing ecosystem functioning at regional to global scales are needed to define essential biodiversity variables to monitor biodiversity status (Pereira et al. 2013; Jetz et al. 2019), to advance in the definition of critical but still unassessed planetary boundary (Steffen et al. 2015; Richardson et al. 2023), and to quantify their associated ecosystem services (Costanza et al. 1997; Balvanera et al. 2017).

There are multiple ways to evaluate ecosystem functioning, from concepts such as species traits or Plant Functional Types (PFTs) to direct observation techniques such as eddy covariance (EC) and remote sensing. Traditionally, studies on ecosystem functioning were approached by grouping species into PFTs based on structural (e.g., biotypes), phylogenetic (e.g., coniferous), or functional species traits (e.g., metabolic pathway) that were linked to biological processes (Lavorel et al. 2002, 2007). For instance, the PFT approach has been widely used in land-cover mapping and dynamic vegetation models to simplify the continuum of species traits into a reduced number of discrete categories suitable for regional-to-global synthesis and modeling studies (Wullschlegel et al. 2014). However, this simplification can lead to information loss (Funk et al. 2017) and may not be capable of predicting the overall ecosystem functioning (Virtanen, 2017; Thomas et al. 2019). Another more recent way to evaluate ecosystem functioning is by using EC (Reichstein et al. 2014; Migliavacca et al. 2021). ~~EC~~ ~~This method~~ uses high-frequency wind and scalar mixing ratio data for calculating the Net Ecosystem CO₂ Exchange (NEE) between the land surface and the atmosphere at the field scale (Baldocchi et al. 2001, 2020). This approach is widely used and regional (e.g., AmeriFlux, AsiaFlux, ICOS, NEON), and a global network of EC measurements has been formed (e.g., FLUXNET) (Franz et al. 2018; Knox et al. 2019). Although FLUXNET has provided unprecedented information on the carbon, water, and energy exchange between the earth's surface and the atmosphere, these measurements still show limitations to assessing ecosystem

73 functioning at regional or global scales due to their small footprints (essentially considered as point-scale data (Chu et al. 2021)
74 and a lack of [spatial](#) representativity (Villarreal et al. 2018, 2021). In parallel, advances in remote sensing are providing new
75 opportunities to quantify ecosystem functioning and functional diversity from regional to global scales (Rocchini et al. 2018;
76 Skidmore et al. 2021). Consequently, combining field-based measurements (e.g., EC) with remote sensing data may allow for
77 better information integration across multiple spatial and temporal scales (Running et al. 1999; Wang et al. 2017). Indeed,
78 multiple studies have aimed to derive global maps combining flux measurements with earth observation data, although
79 challenges and limitations still need to be addressed (e.g., FLUXCOM; Huang et al. 2019; Jung et al. 2020; Liu et al. 2023;
80 Pacheco-Labrador et al. 2023; Gomasasca et al. 2024; Nelson et al. 2024).

81 Ecosystem functioning and functional diversity at the regional scale can be assessed using satellite-derived Ecosystem
82 Functional Types (EFTs) (Paruelo et al. 2001). Conceptually, EFTs are defined as patches of the land surface that share similar
83 dynamics of matter and energy exchanges between the biota and the physical environment (Alcaraz-Segura et al. 2006, 2013;
84 Cazorla et al. 2020, 2021, 2023). The concept of EFT is equivalent to the concept of PFTs but applied to a higher level of
85 biological organization. That is, just like plant species can be grouped based on shared functional traits (e.g., growth rates,
86 nitrogen fixation) into PFTs, ecosystems can be grouped based on their common functional dynamics (e.g., productivity,
87 seasonality, phenology) into EFTs (Paruelo et al. 2001). Remote sensing has been empirically applied to identify EFTs, mainly
88 through spectral indices related to carbon dynamics (Paruelo et al., 2001; Alcaraz-Segura et al., 2006; Ivits et al., 2013), but
89 also incorporating other functional attributes such as evapotranspiration, surface temperature, and albedo (e.g., Fernández et
90 al. 2010; Pérez-Hoyos et al. 2014) or soil characteristics based on their greenhouse gas flux dynamics (Petraakis et al. 2018).
91 [Among these functional attributes, those linked to carbon dynamics, particularly primary production, represent one of the most](#)
92 [integrative dimensions of ecosystem functioning because they reflect the main entry of energy into ecosystems and are directly](#)
93 [related to key carbon and energy exchanges \(Virginia and Wall 2001; Pereira et al. 2013; Xiao et al. 2019\). Moreover, primary](#)
94 [production provides a holistic response to environmental changes and constitutes a synthetic indicator of ecosystem health](#)
95 [\(Costanza et al. 1992; Skidmore et al. 2015\).](#) Other authors have used EFTs to: describe large-scale functional biogeographical
96 patterns (Ivits et al. 2013; Cazorla et al. 2021), assess the representativeness of environmental observatory networks (Villarreal
97 et al. 2018, 2019), assess the ecosystem functional diversity (Alcaraz-Segura et al. 2013; Liu et al. 2023; Armstrong et al. 2024),
98 evaluate the effects of land-use changes on ecosystem functioning (Oki et al. 2012; Domingo-Marimon et al. 2024), improve
99 weather forecasting (Lee et al. 2013; Müller et al. 2014) and species distribution/abundance models (Arenas-Castro et al. 2018,
100 2019), and to identify geographic priorities for biodiversity conservation (Cazorla et al. 2020).

101 So far, EFTs have been identified from satellite remote sensing data. However, whether such top-down-identified EFT classes
102 are biologically meaningful in ecological processes measured on the ground, such as biogeochemical fluxes, remains untested.
103 That is, whether satellite-derived EFT classes differ in their exchanges of energy and matter between ecosystems and the
104 atmosphere. Therefore, linking satellite-derived EFTs identified at large scales to biogeochemical fluxes measured at the site
105 level could help strengthen the ecological significance of the EFT patterns for ecosystem modeling and functional diversity
106 assessments remotely, as it provides empirical evidence for using the concept at these scales.

107 This study aims to provide field-based empirical evidence for using satellite-derived EFTs as descriptors of regional
108 heterogeneity in ecosystem functioning measured on the ground (i.e., seasonal dynamics of NEE). We hypothesize that
109 satellite-derived EFTs classes significantly differ in their exchanges of energy and matter with the atmosphere from each other,
110 in the same way as estimated with in situ field observations. Here, we propose that different satellite-derived EFTs classes
111 display significantly different NEE measurements using the EC technique, while sites under the same EFT should exhibit
112 similar NEE dynamics. To achieve our goal, we used publicly available data across continental Europe, given its high density
113 of EC sites, 1) to characterize the regional patterns of ecosystem functioning using satellite-derived EFTs; 2) to assess whether
114 different satellite-derived EFTs correspond to different NEE dynamics measured on the ground with the EC technique; and 3)
115 to assess how EFTs perform compared to traditional PFTs to discriminate different NEE dynamics.

116 **2 Material and methods**

117 **2.1 Study area**

118 We used NEE information from continental Europe as it has one of the largest densities of EC sites worldwide (Table 1). The
119 sites were distributed across four biogeographical regions (EEA 2016): Mediterranean (12 sites), Continental (21 sites),
120 Atlantic (9 sites), and Alpine (8 sites). Only sites with a long-term (i.e., from 3 to 14 years) NEE time-series were included in
121 the analysis (detailed below).

122

123

124

125

126

127 **Table 1.** Main characteristics of the 50 Eddy Covariance (EC) sites in the study area. Data from FLUXNET 2015 dataset.

ID	Site	Country	PFT	EFT code	Biogeographical region	n years (2001-2014)	Elevation (m)	Latitude	Longitude
AT-Neu	Neustift/Stubai Valley	Austria	Grasslands	Da2	Alpine	11 (2002-2013)	970	47.116	11.317
BE-Bra	Brasschaat (De Inslag Trees)	Belgium	Mixed Trees	Cc1	Atlantic	14 (2001-2014)	16	51.309	4.520
BE-Lon	Lonzee	Belgium	Croplands	Ba1	Atlantic	11 (2004-2014)	167	50.552	4.744
BE-Vie	Vielsalm	Belgium	Mixed Trees	Bc1	Continental	14 (2001-2014)	439	50.305	5.998
CH-Cha	Chamau grassland	Switzerland	Grasslands	Db1	Continental	10 (2005-2014)	393	47.210	8.410
CH-Dav	Davos-Seehorn forest	Switzerland	Evergreen Needleleaf Trees	Ac2	Alpine	14 (2001-2014)	1639	46.815	9.855
CH-Fru	Fruebuel grassland	Switzerland	Grasslands	Da2	Continental	10 (2005-2014)	982	47.115	8.537
CH-Lae	Laegeren	Switzerland	Mixed Trees	Da1	Continental	11 (2004-2014)	689	47.478	8.365
CH-Oe1	Oensingen1 grass	Switzerland	Croplands	Cb1	Continental	7 (2002-2008)	450	47.285	7.731
CH-Oe2	Oensingen2 crop	Switzerland	Croplands	Cb1	Continental	11 (2004-2014)	452	47.286	7.733
CZ-BK1	Bily Kriz-Beskidy Mountains	Czech Republic	Evergreen Needleleaf Trees	Cc1	Continental	11 (2004-2014)	875	49.502	18.536
CZ-BK2	Bily Kriz-grassland	Czech Republic	Grasslands	Ac1	Alpine	9 (2004-2012)	855	49.494	18.542

ID	Site	Country	PFT	EFT code	Biogeographical region	n years (2001-2014)	Elevation (m)	Latitude	Longitude
CZ-wet	CZECHWET	Czech Republic	Wetlands	Ba1	Continental	9 (2004-2012)	426	49.024	14.770
DE-Akm	Anklam	Germany	Wetlands	Ba1	Continental	5 (2010-2014)	-1	53.866	13.683
DE-Geb	Gebesee	Germany	Croplands	Ba1	Continental	14 (2001-2014)	161	51.100	10.914
DE-Gri	Grillenburg-grass station	Germany	Grassland	Da2	Continental	11 (2004-2014)	385	50.949	13.512
DE-Hai	Hainich	Germany	Mixed Trees	Ca1	Continental	12 (2001-2012)	430	51.079	10.452
DE-Kli	Klingenberg	Germany	Croplands	Ba1	Continental	11 (2004-2014)	478	50.892	13.522
DE-Lkb	Lackenberg	Germany	Evergreen Needleleaf Trees	Ab2	Continental	5 (2009-2013)	1308	49.099	13.304
DE-Lnf	Leinefelde	Germany	Deciduous Broadleaf Trees	Da1	Continental	11 (2002-2012)	451	51.328	10.367
DE-Obe	Oberbärenburg	Germany	Evergreen Needleleaf Trees	Ac1	Continental	7 (2008-2014)	734	50.786	13.721
DE-RuR	Rollesbroich	Germany	Grasslands	Da2	Continental	4 (2011-2014)	515	50.621	6.304
DE-RuS	Selhausen Juelich	Germany	Croplands	Cb1	Atlantic	4 (2011-2014)	103	50.865	6.447
DE-Seh	Selhausen	Germany	Croplands	Cb1	Atlantic	4 (2007-2010)	103	50.870	6.449
DE-Spw	Spreewald	Germany	Mixed Trees	Ca1	Continental	5 (2010-2014)	61	51.892	14.033
DE-Tha	Tharandt-Anchor Station	Germany	Evergreen Needleleaf Trees	Bc1	Continental	14 (2001-2014)	385	50.963	13.566

ID	Site	Country	PFT	EFT code	Biogeographical region	n years (2001-2014)	Elevation (m)	Latitude	Longitude
DK-Eng	Enghave	Denmark	Croplands	Ca1	Continental	4 (2005-2008)	10	55.690	12.191
DK-Sor	Soroe-LilleBogeskov	Denmark	Deciduous Broadleaf Trees	Da1	Continental	14 (2001-2014)	40	55.485	11.644
ES-Amo	Amoladeras	Spain	Shrublands	Ad4	Mediterranea	6 (2007-2012)	58	36.833	-2.252
ES-LJu	Llano de los Juanes	Spain	Shrublands	Ad1	Mediterranea	10 (2004-2013)	1600	36.926	-2.752
FR-Fon	Fontainebleau	France	Deciduous Broadleaf Trees	Da1	Atlantic	10 (2005-2014)	103	48.476	2.780
FR-Gri	Grignon	France	Croplands	Cc1	Atlantic	11 (2004-2014)	125	48.844	1.951
FR-LBr	Le Bray	France	Cropland	Cd1	Atlantic	8 (2001 - 2008)	61	44.717	-0.769
FR-Pue	Puechabon	France	Mixed Trees	Cd1	Mediterranea	14 (2001-2014)	270	43.741	3.595
IT-BCi	Borgo Cioffi	Italy	Croplands	Db4	Mediterranea	11 (2004-2014)	20	40.523	14.957
IT-CA1	Castel d'Asso1	Italy	Croplands	Bd1	Mediterranea	4 (2011-2014)	200	42.380	12.026
IT-CA2	Castel d'Asso2	Italy	Croplands	Cb1	Mediterranea	4 (2011-2014)	200	42.377	12.026
IT-CA3	Castel d'Asso3	Italy	Croplands	Bd1	Mediterranea	4 (2011-2014)	197	42.380	12.022
IT-Col	Collelongo-Selva Piana	Italy	Deciduous Broadleaf Trees	Da1	Alpine	14 (2001-2014)	1560	41.849	13.588
IT-Cpz	Castelporziano	Italy	Evergreen Needleleaf Trees	Dd1	Mediterranea	9 (2001-2009)	68	41.705	12.376

ID	Site	Country	PFT	EFT code	Biogeographical region	n years (2001-2014)	Elevation (m)	Latitude	Longitude
IT-Lav	Lavarone (after 3/2002)	Italy	Evergreen Needleleaf Trees	Bc1	Alpine	12 (2003-2014)	1353	45.956	11.281
IT-MBo	Monte Bondone	Italy	Grasslands	Aa1	Alpine	11 (2003-2013)	1550	46.014	11.045
IT-Noe	Sardinia/Arca di Noe	Italy	Shrublands	Ad1	Mediterranea	11 (2004-2014)	25	40.606	8.151
IT-Ren	Renon	Italy	Evergreen Needleleaf Trees	Ac1	Alpine	13 (2001-2013)	1730	46.586	11.433
IT-Ro1	Roccarespamp ani1	Italy	Deciduous Broadleaf Trees	Da1	Mediterranea	8 (2001-2008)	235	42.408	11.930
IT-Ro2	Roccarespamp ani2	Italy	Deciduous Broadleaf Trees	Da1	Mediterranea	11 (2002-2012)	160	42.390	11.920
IT-SRo	San Rossore	Italy	Evergreen Needleleaf Trees	Cd3	Mediterranea	12 (2001-2012)	6	43.727	10.284
IT-Tor	Torgnon	Italy	Grassland	Aa1	Alpine	7 (2008-2014)	1260	45.844	7.578
NL-Hor	Horstermeer	Netherlands	Mixed Trees	Da1	Atlantic	8 (2004-2011)	2	52.240	5.071
NL-Loo	Loobos	Netherlands	Evergreen Needleleaf Trees	Bd2	Atlantic	14 (2001-2014)	25	52.166	5.743

129

130 2.2 Satellite-derived Ecosystem Functional Types (EFTs)

131 To characterize the regional heterogeneity in ecosystem functioning across continental Europe, we identified EFTs based on
132 the 2001-2014 time-series of satellite images of the Enhanced Vegetation Index (EVI) captured by the MODIS-Terra sensor.
133 These images (MOD13Q1.C006 product) provide a maximum composite EVI value every 16 days at a ~230 m spatial
134 resolution. EVI is a proxy for canopy greenness, vegetation carbon gains, or primary production (Huete et al. 1999). Based on
135 the approach by Alcaraz-Segura et al. (2013), we identified EFTs using three biologically meaningful metrics of the EVI
136 seasonal dynamics: the EVI annual mean (EVI_mean; an estimator of annual primary production), the EVI seasonal standard
137 deviation (EVI_SD; a descriptor of seasonality), and the date of maximum EVI (EVI_DMAX; an indicator of phenology). We
138 chose to use MODIS data instead of other satellites with higher spatial resolution (e.g., Landsat or Sentinel-2) because MODIS
139 has several advantages in terms of data availability and quality (e.g. more years of data and cloud-free image every 16-days)
140 along the time series (see S1).

141 The range of values of each EVI metric was divided into four intervals, giving a potential number of 64 EFTs ($4 \times 4 \times 4$). For
142 EVI_DMAX, the four intervals agreed with the four seasons of the year. For EVI_mean and EVI_SD, we extracted the first,
143 second, and third quartiles for each year, ~~and then calculated their interannual average for the 14 years.~~ For each quartile, we
144 calculated the interannual mean of the 14-year period and used them as breaks between classes. These breaks were applied
145 back to each year as the thresholds for EVI_Mean and EVI_sSD to set EFT classes (S2, Table S1). We used this four-class
146 discretization and fixed class boundaries to obtain a coherent and ecologically interpretable classification (Noble and Gitay
147 1996) that applies consistently across years. This approach enables interannual comparisons of spatial functional heterogeneity
148 and maintains continuity with previous EFT implementations (Alcaraz-Segura et al. 2013, Cazorla et al. 2021, 2023).
149 Moreover, recent methodological assessments indicate that EFT derivation is robust to the number of bins used to discretize
150 EF attributes (e.g., Liu et al. 2023). To name EFTs, we used two letters and a number: the first capital letter indicates net
151 primary production (EVI_mean), increasing from A to D; the second small letter represents seasonality (EVI_SD), decreasing
152 from a to d; the numbers are a phenological indicator of the growing season (EVI_DMAX), with values 1-spring, 2-summer,
153 3-autumn, 4-winter (see S3, Table S2 for a schematic summary of code combinations and examples). To summarize the
154 ecosystem functional diversity of the 2001–2014 period, we calculated the dominant EFT (i.e., the mode value for each pixel)
155 of these years.

156 2.3 Eddy covariance (EC) sites for net ecosystem exchange (NEE)

157 To obtain NEE fluxes, 50 EC sites were selected across our study area from the FLUXNET2015 dataset (Table 1). The
158 FLUXNET network (Baldocchi et al. 2001, 2020) provides high-quality, community-based, global data on CO₂, H₂O, and
159 energy exchanges between the biosphere and the atmosphere measured using the EC technique (Baldocchi, 2003). We used
160 data of NEE of CO₂ (NEE_VUT_REF, gC m⁻² d⁻¹) from the FLUXNET2015 database. We selected data from

161 FLUXNET2015 because they are publicly available and offer benefits in terms of standardized methodology. FLUXNET2015
 162 incorporates NEE measurements along with a quality flag based on an annually determined Variable Ustar Threshold (VUT),
 163 which is selected to maximize model efficiency (MEF) (Pastorello et al. 2020). The MEF analysis is repeated for each one of
 164 the half-hourly data (Baldocchi et al. 2001, 2020). We selected sites that: (a) were located in our study area; (b) provided more
 165 than three consecutive years of data over the 2001-2014 period; (c) provided daily averages of NEE calculated from half-
 166 hourly data; and (d) had quality control information (i.e., NEE_VUT_REF data with quality control flag QC > 1 were removed
 167 since they represent medium and poor quality gap-filled data).

168 We applied Discriminant Analysis (DA) to assess whether different satellite-derived EFT classes correspond to different NEE
 169 dynamics and whether sites under the same EFT exhibit similar NEE dynamics (S42). The DA allowed us to examine the
 170 homogeneity within each EFT class and the differences among EFT classes based on the annual dynamics of NEE as a predictor
 171 variable (Williams, 1981, 1983). We selected the EFT where each EC site was located and its corresponding interannual
 172 average of the seasonal cycle of NEE for the available years. EC sites fluxes were regarded as the ground truth standard against
 173 which the satellite data were compared to calculate five performance metrics: Kappa, Accuracy, Precision, Recall, and F1
 174 score (Table 2).

175
 176 **Table 2.** Metrics, interpretations, and equations used to evaluate and compare results from the discriminant analysis, Pr(a) is
 177 the relative observed agreement between observations, and Pr(e) is the hypothetical probability of agreement by chance. True
 178 Positives are correctly classified as positive, True Negative are correctly classified as negative, Positives are all positives
 179 including false positives (i.e., including falsely classified as positive, Type I error) and, Negatives are all negatives including
 180 false negatives (i.e. falsely classified as negative, Type II error). All performance metrics oscillate between 0 (disagreement)
 181 and 1 (maximum agreement).

182

Metric	Meaning	Equation
Kappa	Measures the percentage of data values in the main diagonal of the contingency table and adjusts these values for agreement that could be expected due to chance alone	$K = \frac{\text{Pr}(a) - \text{Pr}(e)}{1 - \text{Pr}(e)}$
Accuracy	Degree of closeness of measurements of a quantity to that quantity's true value	$\text{Accuracy} = \frac{\text{True Positives} + \text{True Negatives}}{\text{Positives} + \text{Negatives}}$

Precision	Fraction of relevant instances among the retrieved instances (also called positive predictive value, i.e., how many EFTs were well discriminated)	$\text{Precision} = \text{True Positives} / (\text{True Positives} + \text{False Positives})$
Recall	Fraction of relevant instances that have been retrieved over the total amount of relevant instances	$\text{Recall} = \text{True Positives} / (\text{True Positives} + \text{False Negatives})$
F1	Considers both the Precision and the Recall of the test to compute the score	$\text{F1 score} = 2 \times (\text{Precision} \times \text{Recall}) / (\text{Precision} + \text{Recall})$

183

184 2.4 Comparing how EFTs and PFTs discriminate different NEE dynamics

185 The PFT corresponding to each EC site was assigned by each of their principal investigators using the International Geosphere-
186 Biosphere Programme (IGBP, 1992). Subsequently, we verified the assigned PFTs using the MODIS MCD12Q1 land cover
187 product. The PFT categories present in the EC sites were: cropland (15 sites), deciduous broadleaf trees (6), evergreen
188 needleleaf trees (10), grassland (6), mixed trees (7), shrubland (3), and wetland (1) (Table 1).

189 During the comparison of the performance of PFTs and EFTs to discriminate the seasonal dynamics of NEE, we considered
190 the unbalanced sample size due to the different number of classes of EFTs (18) and PFTs (7) represented by FLUXNET2015
191 and the different number of EC sites per PFT class (which ranged between 3 and 31). To do this, we performed the following
192 steps:

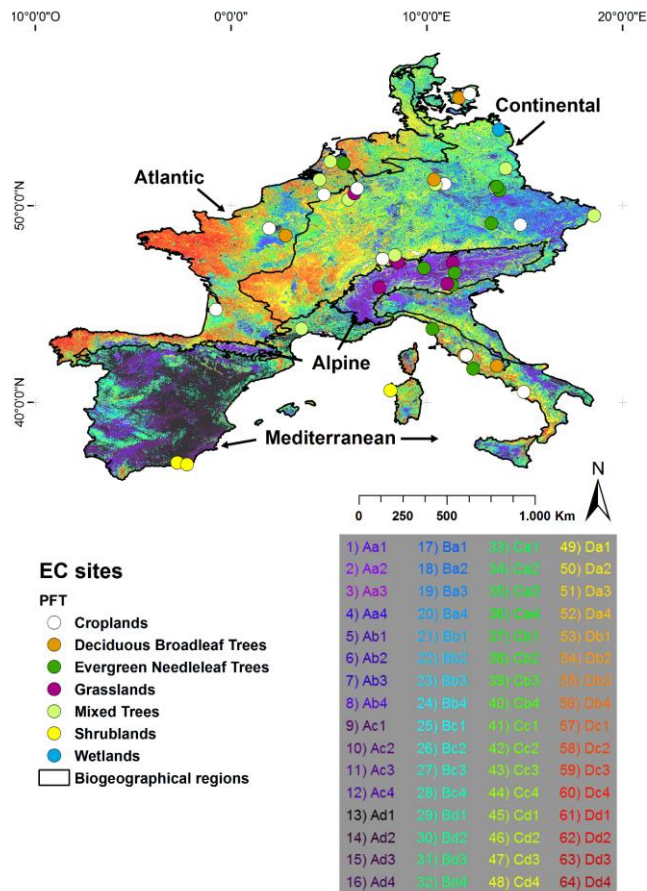
193 First, we calculated all possible combinations (C) without repetitions between the 18 EFT and the 7 PFT classes ($C(18,7) =$
194 31834). Second, since the DA needs balanced data, we discarded all combinations with different numbers of EC sites in the
195 combined EFT and PFT classes. Third, for each combination, we applied discriminant analysis to assess how the EFT and PFT
196 classifications performed to discriminate the seasonal dynamics of NEE. For each discriminant analysis, we obtained five
197 metrics of performance (Table 2). Fourth, to assess whether significant differences existed in the performance metrics between
198 EFTs and PFTs, we applied the Wilcoxon non-parametric test. For each combination of a number of classes and EC sites, there
199 was a different number of discriminant analyses in the EFT subset and the PFT subset (S42 Table S33). To account for such
200 an unbalanced design during the Wilcoxon test, we fixed the sample size to the smaller subset (either from the EFT or the PFT
201 classification) and randomly bootstrapped the performance metrics from the bigger one. Fifth, we calculated the mean and
202 standard deviation of each metric obtained by the EFTs and PFTs classifications, the average p-value, and the percentage of
203 times we obtained significant differences (p-value <0.05) between EFTs and PFTs.

3 Results

3.1 Regional heterogeneity in ecosystem functioning using satellite-derived EFTs

The map of the EVI-derived proxies of productivity (EVI_mean), seasonality (EVI_SD), and phenology (DMAX) (S53 Fig. S1a-c) and their integration into EFTs (Fig. 1) provided a characterization of the spatial patterns of our focal ecosystem function across Europe. At the continental scale, productivity decreased eastwards and southwards (Fig. 1, S53 Fig. S4). Seasonality was greater in cultivated and mountain grassland areas (Fig. 1, S53 Fig. S5), and the most frequent EVI maxima occurred in spring and summer (Fig. 1, S53 Fig. S6).

The greatest EVI_mean (D) was reached in the Atlantic and Continental biogeographic regions (Fig. 1, S53 Fig. S4d). At the same time, the lowest EVI_mean (A) occurred in the western part of the Mediterranean region, corresponding to most of the Iberian Peninsula, some parts of the Italian Peninsula, the mountainous areas of the Alpine region, and in the eastern part of the Continental region (Fig. 1, S53 Fig. S4a). The greatest seasonality (a) occurred in the highest altitudes of the Alpine region (peaks of Alps <3000 meters), the Continental region (southwestern, northwestern, and eastern part of this region), and the eastern part of the Atlantic region (Fig. 1, S53 Fig. S5a). The lowest seasonality (d) was observed in the western part of the Mediterranean region, specifically in the Iberian Peninsula, the Gulf of Lion's surroundings, and the Atlantic region's Coastal western places (Fig. 1, S53 Fig. S5d). The phenological indicator of the growing season, DMAX, showed that most areas of the Mediterranean region have the EVI maxima in spring (1). EVI maxima in spring (1) were also observed in the Continental and Alpine regions (Fig. 1, S53 Fig. S6a). Maxima in summer (2) were identified in western places of the Atlantic and most of the Alpine regions (Fig. 1, S53 Fig. S6b). EVI maxima in autumn (3) mainly in the Mediterranean region (Fig. 1, S53 Fig. S6c). Maxima in winter (4) were rare and emerged in the eastern part of the Atlantic region, where the maximum productivity was found and in the western part of the Mediterranean region (Fig. 1, S53 Fig. S6d). [A simplified representation of the EFT map, obtained by clustering EFTs based on their functional similarity, is provided in the Supplementary Material \(S6\).](#)



225

226

227

228

229

230

231

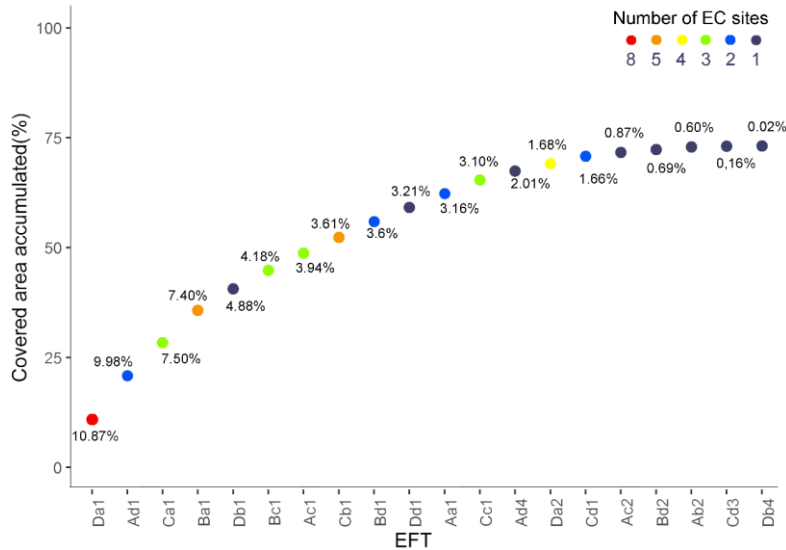
232

Fig. 1. Ecosystem Functional Types (EFTs) based on MODIS-EVI dynamics (~230 m resolution) and Eddy Covariance (EC) sites corresponding to the 2001–2014 period. Capital letters in the legend correspond to the EVI annual mean (EVI_mean) level, ranging from A to D for low to high productivity. Small letters show the seasonal standard deviation (EVI_SD), ranging from a to d for high to low seasonality of carbon gains. The numbers indicate the season when the maximum EVI took place (DMAX): (1) spring, (2) summer, (3) autumn, (4) winter. Places with EC sites are indicated shown with colored circles squared colors, where each one color represents a different plant functional type (PFT). Biogeographical regions are based on the official European biogeographical regions map (EEA, 2016) and are represented by black lines.

233 **3.2 Ground-based NEE of the satellite-derived EFTs**

234 In total, 20 of the 64 potential EFTs, containing 73.10 % of our study area, were represented by the network of the 50 long-
 235 term EC sites that met our selection criteria (Fig. 2). The most abundant EFT, Da1, showed high productivity (D), high
 236 seasonality (a), and maximum EVI in spring (1) (Fig. 2). Da1 occupied 10.87% of the surface and was distributed throughout
 237 the study area but abundantly in the western and southern extremes of the Atlantic Region). Da1 was represented by 8 EC sites
 238 that exhibited NEE with a strong seasonal variability, with a pronounced peak of carbon assimilation between -7.23 and -7.46
 239 g C m⁻² d⁻¹ in spring (Fig. 4) and corresponded with the most abundant ecosystem in Europe, the Deciduous Broadleaf and
 240 Mixed Forest (S42 Table S42). The second most abundant EFT, Ad1, showed low productivity (A), low seasonality (d), and
 241 maximum EVI also in spring (1). Ad1 occupied 9.98% of the territory, mainly in the Iberian Peninsula (Fig. 1). Ad1 was
 242 represented by 2 EC sites (Fig. 2) that exhibited NEE dynamics with low seasonality and the peak of carbon assimilation
 243 (NEE) between -0.72 and -1.98 g C m⁻² d⁻¹ in spring (Fig. 4) and was concentrated in areas dominated by shrub vegetation
 244 (S42 Table S42).

245



246

247 **Fig. 2.** Accumulated area covered by the Ecosystem functional types (EFTs; in %) represented in the study (ordered from
 248 highest to lowest). Colors indicate the number of eddy covariance (EC) sites, and the numbers indicate the area occupied by
 249 each of these EC sites (in %).

250

251 Regarding the abundance of EC sites, the EFT Da1 mentioned above was represented by 8 EC sites, followed by EFT Ba1 and
252 Cb1 with 5 EC sites. The EFT Ba1, was also abundant, occupying 7.4% of the total surface (Fig. 2), and was located mainly
253 in the eastern part of the study area (Atlantic and Continental regions) (Fig. 1). The EFT Cb1, was less abundant than the
254 previous one (3.61%) and was located in central areas of the Atlantic and Continental regions. NEE dynamics were
255 characterized by high (a) and medium-high (b) seasonality and the peak time of carbon assimilation between -6.40 and -7.53
256 g C m⁻² d⁻¹ in spring. In both cases, these places corresponded with cereal crops (S42 Table S42).
257 Our discriminant analysis showed that EFTs significantly differed in NEE measured in situ with the EC technique. The average
258 of the performance metrics obtained from the discrimination that satellite EFTs made of EC site NEE ranged between 0.953
259 to 0.978 (Table 3a). NEE dynamics significantly differed between different EFTs but were similar within the same EFTs (S53
260 Fig. S2). For example, the EFT “Da1”, which had high productivity, high seasonality, and spring EVI maxima, also showed
261 high average NEE values, high seasonality in NEE, and maximum carbon assimilation in spring (Fig. 4, EC sites DE-Lnf, FR-
262 Fon). The EFT “Bc1”, with medium to high productivity, medium seasonality, and spring EVI maxima, was also characterized
263 by moderate seasonality in terms of NEE and maximum carbon assimilation in spring (Fig. 4a for EC sites BE-Vie, DE-Tha).
264 Contrary, the EFT “Ad1”, which had low productivity, low seasonality, and EVI spring maxima, also showed low average
265 NEE, low seasonality in NEE, and a peak of maximum carbon assimilation in spring (ES-Lju, IT-Noe). As another example,
266 the EFT “Cb1”, with medium productivity, medium-high seasonality, and spring EVI maxima, also showed medium to high
267 seasonality in terms of NEE and maximum carbon assimilation in spring (Fig. 4a for EC sites DE-she, DE-RuS).

268 3.3 Comparison between EFTs and PFTs to discriminate NEE measured by EC

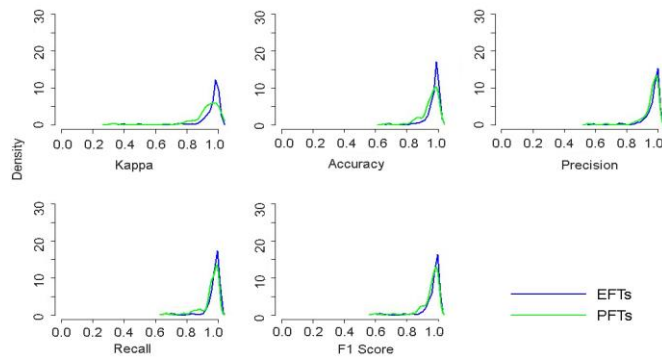
269 EFTs performed marginally better than PFTs in capturing differences in NEE dynamics measured on the ground (Table 3).
270 The average across all discriminant analyses in all performance indices was marginally but not significantly higher for EFTs
271 (e.g., mean Kappa = 0.953) than for PFTs (e.g., mean Kappa = 0.923) (Table 3, Fig. 3); However, the standard deviation (s.d.)
272 across all discriminant analyses was higher for PFTs (e.g., s. d. of Kappa = 0.078) than for EFTs (e.g., s. d. of Kappa = 0.067).
273 No significant differences between the performance metrics of EFTs and PFTs were detected by the Wilcoxon-test in any of
274 the indices (Table 3).

275
276
277
278
279 **Table 3.** Mean performances metrics, their standard deviation (SD) and differences in: Kappa, Accuracy, Precision, Recall
280 and F1 values obtained from discriminant analysis of combinations with equal number of classes and EC sites of (a) ecosystem
281 functional types (EFTs) and (b) plant functional types (PFTs). To assess for significant differences, we applied a Wilcoxon-

282 test (p-values showed), and we calculated the percentage of cases in which differences between EFTs or PFTs with NEE were
 283 significant (% sig), in this case, none.

284

	a. EFTs		b. PFTs		Difference	
	mean	SD	mean	SD	p-value	% sig
Kappa	0.953	0.067	0.923	0.078	1	0
Accuracy	0.972	0.040	0.952	0.051	1	0
Precision	0.967	0.047	0.959	0.057	1	0
Recall	0.978	0.033	0.960	0.040	1	0
F1	0.972	0.040	0.959	0.048	1	0



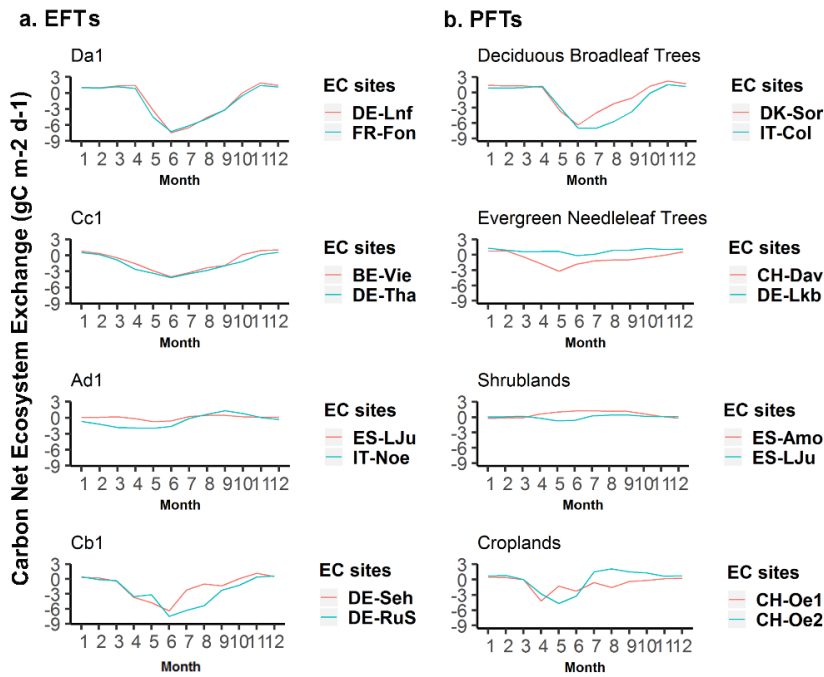
285

286 **Fig. 3.** Histograms of performances from discriminant analysis for all combinations of Ecosystem Functional Types (EFTs)
 287 and Plant Functional Types (PFTs) with equal number of classes and EC sites. Blue lines correspond to EFTs and green lines
 288 to PFTs.

289

290 In general, NEE dynamics were similar for the same PFT or EFT across EC sites (Fig. 4), though there were some exceptions
 291 for certain PFTs (Fig. 4b; S53 Fig. S3). Sites corresponding to the PFT “deciduous broadleaf trees” or the EFT “Da1” always

292 showed similar NEE (Fig. 4; Table 1). However, for the PFT “evergreen needleleaf trees”, NEE dynamics exhibited a different
 293 seasonality and variable maximum carbon assimilation across sites (Fig. 4b for EC sites CH-Dav, DE-Lkb). Differences in
 294 NEE dynamics across sites were also observed for shrublands where the ES-LJu site (EFT Ad1) was assimilating carbon
 295 throughout the year, particularly in spring, while the ES-Amo site (EFT Ad4) was mainly emitting carbon throughout the year
 296 except for winter. Larger differences in NEE occurred in the PFT croplands, with maximum carbon sequestration occurring
 297 in different seasons (Fig. 4b, for sites CH-Oe1 and CH-Oe2 (EFT Cb1)).
 298



299
 300 **Fig. 4.** Comparison of the variability within and across classes of Ecosystem Functional Types (EFTs) and Plant Functional
 301 Types (PFTs) in the seasonal dynamics of NEE. a) Variability inter EFTs: annual mean of NEE dynamics from different places

302 randomly selected with the same EFT; and b) variability inter PFTs and intra EFTs: annual mean of NEE dynamics from
303 different places with the same PFT and different EFT.

304 **4 Discussion**

305 Remotely-sensed EFTs successfully mapped functionally homogeneous land patches regarding NEE dynamics measured in
306 situ with the EC technique. Furthermore, EFTs performed at least similarly to the commonly used PFTs for discriminating
307 among different NEE seasonal dynamics (Table 3). EFTs have the advantage of being more sensitive in their responses to
308 short-term changes in ecosystem functioning than the slower-responding plant community composition or canopy structure.
309 Furthermore, they ~~and~~ can be recalculated on an annual basis using the same classification rules, which provides a
310 straightforward way to track interannual changes in ecosystem functioning (Müller et al. 2014). Our focal ecosystem function
311 was NEE dynamics, which is related to primary production (but also to ecosystem respiration), one of the most essential and
312 integrative descriptors of ecosystem functioning (Virginia and Wall, 2010). Hence, satellite-derived EFT classifications could
313 be used to monitor the status and changes of the regional heterogeneity or spatial diversity of the essential variable of ecosystem
314 productivity as a surrogate of the overall ecosystem performance (Jax, 2010; Pettorelli et al., 2016).

315 **4.1 EFTs capture differences in NEE**

316 EFTs quantified and mapped the spatio-temporal characteristics of carbon dynamics, a crucial aspect for biodiversity
317 conservation and ecosystem services maintenance in a global change context (Midgley et al. 2010). Twenty of the 64 EFTs
318 identified in Europe (corresponding to 73% of the study area) were represented by at least one EC site in the FLUXNET2015
319 dataset with at least three years of data. This number of site-years and the covered area provided sufficient evidence to confirm
320 the validity of the EFT concept. Therefore, our approach could help to assess carbon dynamics at a regional scale by providing
321 homogeneous land areas in terms of their primary production dynamics (Running et al. 2004, Zhang et al. 2015). This fact
322 helps to understand the regional patterns and drivers of the differences in carbon dynamics at the regional scale and could
323 contribute to reducing the uncertainties in the global carbon balance (Beer et al. 2010).

324 EFTs capture spatial differences in NEE seasonal dynamics equally well or marginally better than other mainstream
325 approaches, such as PFTs. Different areas may respond differently to environmental changes despite being dominated by the
326 same PFT, and frequently, ecosystem-process models (parameterized for a specific PFT) may not be able to represent these
327 differential responses (Vargas et al. 2013). Usually, the parameterization of a particular PFT is homogeneous within such PFT
328 and does not change, for instance, according to the eco-physiological status of a specific area or its intrinsic plasticity (Müller
329 et al. 2014). In addition, land-cover maps based on a PFT concept are static and difficult to update (i.e., PFT database structure
330 and assumptions are not easily adapted to new data). At the same time, EFTs are a data-driven classification through which
331 we can annually obtain new data and detect changes in the exchange of matter and energy between the ecosystems and the
332 atmosphere in response to environmental variability. In this sense, the literature (Bret-Harte et al. 2008; Suding et al. 2008;

333 Clark et al. 2016; Saccone and Virtanen 2017; Thomas et al. 2018) has pointed out that the PFT approach is not straightforward
334 enough to represent ecosystem functional properties at the ecosystem level.

335 EFTs derived in this study rely on EVI-based attributes, which primarily represent the dynamics of primary production. This
336 focus is consistent with the fact that vegetation greenness and light absorption are tightly linked to APAR, GPP and NEE (e.g.
337 Huete et al. 1997; Running et al. 2004; Shi et al. 2017), making EVI a direct and widely used indicator of ecosystem functional
338 behaviour at large scales. The strong agreement between our EFTs and in situ NEE patterns confirms that EVI captures the
339 dominant functional axis related to carbon uptake. Although additional attributes associated with water or energy fluxes (e.g.,
340 NDWI, land-surface temperature or albedo) could enrich multidimensional EFT frameworks in the future, the carbon-related
341 dynamics encoded in EVI already provide a robust and ecologically meaningful foundation for functional ecosystem
342 classification.

343 **4.2 EFT spatial patterns and environmental controls**

344 EFTs allowed us to characterize the regional heterogeneity of ecosystem functioning across Europe. In relation to the three
345 descriptive attributes of ecosystem functioning from which the EFTs were constructed (EVI_mean; an estimator of primary
346 production, EVI_SD; a descriptor of seasonality and EVI_DMAX; an indicator of phenology), we found general patterns
347 determined by the combination of vegetation characteristics and environmental controls. The role of environmental variables
348 (abiotic and biotic) that control ecosystem processes differ according to the level of biological organization and the spatial
349 scale considered (Reed et al. 1993; Pearson and Dawson, 2003). Ecosystem functioning in natural areas are known to be mainly
350 driven by precipitation (Lauenroth et al. 1978), temperature (Rosenzweig and Dickinson 1968; Jobbagy et al. 2002), soil
351 characteristics (NoyMeir 1973), and vegetation structure (Epstein et al. 1998). In this case, EFTs productivity decreased from
352 east to west influenced by rainfall patterns determined by the Gulf Stream and the distance from the ocean (Palter 2015), which
353 also determines changes in vegetation. Regarding the seasonality of EVI, it increased in relation to two factors: 1) the altitude,
354 having the highest values of seasonality in the mountainous areas (influenced by changes in precipitation, temperature, and
355 consequently, in vegetation), and; 2) the crop areas, where management practices, harvests, and crop changes are responsible
356 of this dynamic and therefore it cannot be explained by natural environmental controls alone. Peaks of maximum EVI in
357 Europe took place in spring and summer when the availability of water (precipitation) and energy (temperature) for vegetation
358 was at its optimum (Whittaker et al. 2003).

359 Boundaries of the biogeographical regions (EEA 2016) were consistent with the EFTs (Fig. 1). Still, while the classification
360 from EEA is static, EFTs provide a data-driven classification that could be better coupled to ecosystem functioning. The Alpine
361 region was dominated by EFTs with low productivity, high seasonality, and maxima in summer. In the high mountain peaks
362 (<3000 meters), the vegetation was reduced to a low density of highly adapted plants that can tolerate extreme conditions (i.e.,
363 the short growing period and fluctuating air temperatures, and therefore, has low productivity, also detected in the global
364 primary productivity patterns of Beer et al. (2010) and Zhang et al. (2017)). In the highest altitudes, snow is present over most

365 of the year, leaving only a short period for the development of the plants, mainly in summer, leading to a summer maximum
366 and a high seasonality (Sundseth, 2009a).

367 A high heterogeneity of EFTs characterized the Mediterranean region due to their high habitat diversity (i.e., high mountains
368 and rocky shores, thick scrub and semi-arid steppes, coastal wetlands, and sandy beaches, constituting a global biodiversity
369 hotspot (Myers et al. 2000)). The main driver of ecosystem functional diversity is the climate (characterized by hot, dry
370 summers and cool winters) (Lionello et al. 2006), in combination with human influence, (i.e., livestock grazing, forest
371 cultivation, and forest fires) (Blondel and Aronson, 1999).

372 The Atlantic region was characterized by EFTs with high productivity, high seasonality, and maximum greening in spring due
373 to the mild winters, cool summers, predominantly westerly winds, and moderate rainfall throughout the year (Hurrell, 1995).
374 These conditions favor non-water-limited deciduous species with high productivity, resulting in a high seasonality. Due to the
375 anthropogenic influence, agricultural landscapes are widespread in this region, one of Europe's five major agricultural regions,
376 according to Kostrowicki (1991). Thus, the region's high productivity must be partly attributed to irrigation, and high
377 seasonality is driven by harvest and cropping cycles.

378 Finally, in the Continental region, the ecosystem's functioning varied largely in terms of productivity, reflecting regional
379 climatic patterns. In the eastern part of the continental region, extremes of hot and cold temperatures and wet and dry conditions
380 are more frequent and strongly impact ecosystem functioning (dominant EFT was Aa1, low productivity, high seasonality, and
381 maximum in spring). These areas are mountainous and experience sub-alpine conditions. Moving west, the climate is
382 characterized by relatively small temperature fluctuations due to the buffering effect of the nearby ocean and the flat landscape
383 (Da1 and Ca1 in the transition) (Sundseth, 2009b).

384 4.3 Opportunities and limitations of EFTs

385 Since EFTs describe ecosystem functioning on an annual basis in homogeneous patches on the land surface, they offer
386 opportunities for application in ecology and conservation compared to approaches that do not represent short-term dynamics
387 (such as PFTs). ~~However, they also have some limitations-~~

388 The concept of EFT has been highlighted as “the first serious attempt to group ecosystems (at large scales) based on shared
389 functional behavior” (Mucina, 2019), and its strength for being applied as a classification scheme is determined by its ability
390 to translate ecosystem functions into discrete entities that can be mapped. EFTs are identified by remote sensing tools from
391 aggregated measurements of ecosystem functions at the pixel level, which, in practice, represents information on the
392 performance of the whole ecosystem at that grain scale. Having the possibility of mapping entities (EFTs) that reflect the
393 principal performance of the entire ecosystem opens a straightforward, tangible, and biologically meaningful way to quantify
394 distributions of ecosystem functions at the regional scale, complementing our traditional view of ecosystems (Paruelo et al.
395 2001; Butchart et al. 2010; Asner et al. 2017). Specifically, satellite-derived dynamic functional classifications, such as EFTs,
396 have several advantages over other static approaches, such as PFTs. Satellite-derived EFAs and EFTs 1) are capable of
397 capturing differences in ecosystem processes as measured in the field; 2) they provide a valuable framework for understanding

398 the mechanisms underlying large-scale ecological changes (Cabello et al. 2016; Alcaraz-Segura et al. 2017; Requena-Mullor
399 et al. 2017, 2018; Arenas-Castro et al. 2018; Lourenço et al. 2018; Vaz et al. 2018); 3) they offer a faster response than
400 compositional or structural approaches to environmental changes (McNaughton, 1989; Mouillot et al. 2013), which are
401 particularly noticeable at the ecosystem level (Vitousek, 1994); 4) they can be more easily monitored and updated than
402 structural or compositional ones under a common protocol in space and time, at different spatial scales and over large
403 extents (Paruelo et al. 2001); 5) they can complement information on vegetation structure and composition (e.g., canopy
404 architecture, vegetation type, PFT), because they constitute complementary dimensions of biodiversity complexity (Noss,
405 1990); 6) they facilitate the direct assessment of ecosystem functions and services (Costanza et al. 2006; Hellmann et al. 2017)
406 and would link critical dimensions of biodiversity to ecosystem processes including the carbon cycle, the water cycle and the
407 provisioning of ecosystem services; 7) they have already been proposed as essential variables for monitoring biodiversity
408 (Pettoirelli et al. 2016; Skidmore et al. 2021).

409 Our approach, as with any other ecosystem classification framework, is still subject to some challenges. First, EFTs represented
410 by several EC sites could be parameterized in terms of NEE dynamics, though not all EFTs (18%) are represented yet.
411 Nevertheless, the subset of EFTs covered by multiple EC sites spans the dominant functional types across Europe, providing
412 a solid empirical basis for validating the classification. Second, the footprint or spatial resolution of the EC measurements
413 varies depending on the micrometeorological conditions (wind direction, wind speed, atmospheric stability) and the ratio of
414 measurement to vegetation height, e.g., forest flux footprints are generally larger than grassland footprints (oscillates between
415 50 m and 200 m) (Schmid 1997; Kljun et al. 2015). In contrast to comparison, the MODIS pixels used have a constant spatial
416 resolution of ~231 m, generating an unavoidable scale mismatch. However, because EC towers are typically
417 placed in relatively large and functionally homogeneous land patches (Aubinet et al. 2012), the MODIS pixel and the flux
418 footprint generally sample comparable surfaces, limiting the practical impact of this mismatch on the regional-scale patterns
419 captured by our EFTs. Nonetheless, we acknowledge that some challenges regarding spatial representativeness remain (Chu
420 et al. 2021). Future studies may reduce this mismatch by using higher-resolution sensors such as Sentinel-2. Such limitations
421 could be handled in future works using satellites with higher spatial resolution, such Sentinel-2 (10 m/pixel), but currently is
422 not possible because the time period of Sentinel-2 data is not covered by FLUXNET data (i.e., Sentinel-2 starts taking data in
423 2015 and the available FLUXNET 2015 database goes up to this year). Alternatively, footprint modelling could be applied
424 when appropriate micrometeorological data exist, but footprint-weighted averaging was not feasible in our study because daily
425 or sub-daily footprint estimates are unavailable for most FLUXNET sites and years, a limitation commonly acknowledged in
426 previous RS-flux integration studies (Chu et al. 2021). Third, different ecosystems regarding other functional aspects (e.g.,
427 evapotranspiration, heat exchange) can be classified here as the same EFT from the NEE dynamics, as we used it as our
428 focal function. However, EFTs could also be identified to characterize the spatiotemporal heterogeneity of multiple ecosystem
429 processes and functions at different scales, including other functional aspects (e.g., albedo, evapotranspiration, heat exchange)
430 (Fernandez et al. 2010). Also other temporal metrics, such as daily anomalies or interannual variability can provide
431 complementary information on short-term or year-to-year ecosystem responses, but they are not expected to improve the

432 discrimination among EFTs, which is intrinsically based on intra-annual functional patterns. Similarly, additional phenological
433 transition metrics such as the start and end of the season (SOS/EOS) may offer complementary insights into growing-season
434 timing and duration; however, their higher sensitivity to noise and temporal gaps, particularly in 16-day MODIS time series,
435 makes peak-greenness metrics like EVI_DMAX more robust and comparable for regional-scale functional classifications.

436 Finally, incorporating EFTs into earth system models is challenging since these models generally use simple and few small
437 numbers of categories in a variable, and some models might not be able to run with so many (64) EFT categories. Nevertheless,
438 some studies have successfully incorporated EFTs into earth system models (Lee et al. 2013; Müller et al. 2014). The
439 incorporation of these types of variables (dynamic and easily accessible) into the models might be helpful in the monitoring
440 and sustainable management of carbon reservoirs at short to medium-time scales.

441 **5 Conclusion**

442 Satellite-derived EFTs are an ecosystem functional classification built from satellite observations of radiation exchanges
443 between the land surface and the atmosphere that allow the identification of homogeneous land patches in terms of an essential
444 ecosystem function, e.g., NEE dynamics, measured on the ground by means of which is related to ecosystem productivity.
445 EFTs performed as well as PFTs in discriminating different NEE dynamics, EFTs, however, have two main advantages: they
446 can be easily updated for any region of the world at an annual frequency based on available satellite information, and EFTs
447 maps are more sensitive to environmental changes than vegetation composition or structure.

448 Our results showed the capability of using ecosystem functional attributes for grouping ecosystems at large scales according
449 to their different net carbon flux dynamics. Such classification, based on the essential biodiversity variable of ecosystem
450 production as a focal ecosystem function, opens the possibility of assessing and monitoring ecosystem functional diversity,
451 the spatial heterogeneity in ecosystem functioning, and carbon-related ecosystem services at regional to global scales.
452 Therefore, our study demonstrates that satellite-derived EFTs provide a valid tool to assess and monitor ecosystem functioning
453 with potential applications in ecosystem monitoring and modeling and biodiversity and carbon management programs.

454 **Data availability**

455 The MODIS database used in this work is maintained by NASA (satellite Terra, sensor MODIS, product MOD13Q1.006) and
456 is mirrored by Google on the Earth Engine servers ([https://developers.google.com/earth-
457 engine/datasets/catalog/MODIS_006_MOD13Q1](https://developers.google.com/earth-engine/datasets/catalog/MODIS_006_MOD13Q1)). FLUXNET2015 eddy covariance data are available through the
458 FLUXNET [website \(https://fluxnet.org/data/fluxnet2015-dataset\)](https://fluxnet.org/data/fluxnet2015-dataset). The Google Earth Engine code used to derive Ecosystem
459 Functional Types (EFTs) is openly available at <https://doi.org/10.5281/zenodo.7524973>. The plant functional types (PFTs)
460 used in this study are based on the IGBP-DIS global 1 km land cover data set "DISCover": proposal and implementation plans,
461 IGBP-DIS available at https://daac.ornl.gov/ISLSCP_II/guides/edc_landcover_xdeg.html.

464 **Author contributions**

465 DAS, AM, JC, JP and BPC designed the study, AM and DAS coordinated it. BPC processed the data and prepared the
466 manuscript with contributions from all authors. BPC and JML prepared the final Fig.s. LM, AK, LS, BG, JD, LŠ, AI, GW,
467 EP, KF, AM, MP, LM, LH, PD, IG, and KP provided FLUXNET data. All authors reviewed the article and provided valuable
468 feedback, especially RV and JML.

469

470 **Competing interests.** Some authors are members of the editorial board of journal Biogeosciences.

471 **Acknowledgements.** This publication is part of the EVEREST project (PID2023-151939OB-I00) funded by
472 MICIU/AEI/10.13039/501100011033 and by ERDF/EU. Funds were also provided by ERDF and Spanish MINECO (project
473 CGL2014-61610-EXP) and to B.C. by University of Almería (PhD contract: research training program). This research was
474 also supported by the project “Earth observations for the characterisation and monitoring of ecosystem functioning in Sierra
475 Nevada (Spain)” (C-EXP-074-UGR23), which has been co-funded by the 2014-2020 FEDER Program and the Consejería de
476 Economía, Conocimiento, Empresas y Universidad of the Andalusian Government; ECOPOTENTIAL, which received
477 funding from the European Union’s Horizon 2020 Research and Innovation Program under grant agreement No. 641762, and
478 the NASA 2016 GEOBON Work Programme Grant # 80NSSC18K0446. EarthCul (reference PID2020-118041GB-I00),
479 funded by the Spanish Ministry of Science and Innovation, Smart-EcoMountains, LifeWatch-ERIC action line, within the
480 Workpackages LifeWatch-2019-10-UGR-01_WP-8, LifeWatch-2019-10-UGR-01_WP-7, and LifeWatch-2019-10-UGR-
481 01_WP-4. Additional support was provided by the “Plan Complementario de I+D+i en Biodiversidad (PCBIO)” through the
482 covey Plan - NextGenerationEU, the Spanish Ministry of Science, and the Regional Government of Andalusia (PID2022–
483 140092OB-I00, MCIN/AEI/FEDER, UE). This work used eddy covariance data acquired and shared by the FLUXNET
484 community. The ERA-Interim reanalysis data are provided by ECMWF and processed by LSCE. The FLUXNET eddy
485 covariance data processing and harmonization was carried out by the European Fluxes Database Cluster, AmeriFlux
486 Management Project, and Fluxdata project of FLUXNET, with the support of CDIAC and ICOS Ecosystem Thematic Center,
487 and the OzFlux, ChinaFlux and AsiaFlux offices. JML was funded by the Plan Propio de Investigación (P9) of the University
488 of Granada. AM was ~~supported~~ funded by the Deutsche Forschungsgemeinschaft (DFG, German Research Foundation) under
489 Germany’s Excellence Strategy – EXC 2070 – 390732324. LM acknowledges the funding provided by Forest Services,
490 Autonomous Province of Bolzano. LŠ acknowledges support from the Ministry of Education, Youth and Sports of the Czech
491 Republic within the CzeCOS program (grant number LM2023048) and the AdAgriF project (CZ.02.01.01/00/22
492 008/0004635).

493

494 **References**

- 495 Alcaraz, D., Paruelo, J., and Cabello, J.: Identification of current ecosystem functional types in the Iberian Peninsula, *Glob.*
496 *Ecol. Biogeogr.*, 15, 200–212, <https://doi.org/10.1111/j.1466-822X.2006.00215.x>, 2006.
- 497 Alcaraz-Segura, D., Paruelo, J. M., Epstein, H. E., and Cabello, J.: Environmental and human controls of ecosystem
498 functional diversity in temperate South America, *Remote Sens.*, 5, 127–154, <https://doi.org/10.3390/rs5010127>, 2013.
- 499 Arenas-Castro, S., Gonçalves, J., Alves, P., Alcaraz-Segura, D., and Honrado, J. P.: Assessing the multi-scale predictive
500 ability of ecosystem functional attributes for species distribution modelling, *PLoS ONE*, 13, e0199292,
501 <https://doi.org/10.1371/journal.pone.0199292>, 2018.
- 502 Armstrong, A., Alcaraz-Segura, D., Reynolds, M., and Epstein, H.: Ecosystem functional types of the circumpolar Arctic
503 tundra based on the seasonal dynamics of vegetation productivity, *Environ. Res. Ecol.*, 3, 025003,
504 <https://doi.org/10.1088/2752-664X/ad4beb>, 2024.
- 505 Arenas-Castro, S., Regos, A., Gonçalves, J. F., Alcaraz-Segura, D., and Honrado, J.: Remotely sensed variables of
506 ecosystem functioning support robust predictions of abundance patterns for rare species, *Remote Sens.*, 11, 2086,
507 <https://doi.org/10.3390/rs11182086>, 2019.
- 508 Asner, G. P., Martin, R. E., Knapp, D. E., Tupayachi, R., Anderson, C. B., Sinca, F., Vaughn, N. R., and Llactayo, W.:
509 Airborne laser-guided imaging spectroscopy to map forest trait diversity and guide conservation, *Science*, 355, 385–389,
510 <https://doi.org/10.1126/science.aaj1987>, 2017.
- 511 Baldocchi, D. D.: Assessing the eddy covariance technique for evaluating carbon dioxide exchange rates of ecosystems: past,
512 present and future, *Glob. Change Biol.*, 9, 479–492, <https://doi.org/10.1046/j.1365-2486.2003.00629.x>, 2003.
- 513 Baldocchi, D. D.: How eddy covariance flux measurements have contributed to our understanding of Global Change
514 Biology, *Glob. Change Biol.*, 26, 242–260, <https://doi.org/10.1111/gcb.14807>, 2020.
- 515 Baldocchi, D., Falge, E., Gu, L., Olson, R., Hollinger, D., Running, S., Anthoni, P., Bernhofer, C., Davis, K., Evans, R., et
516 al.: FLUXNET: A new tool to study the temporal and spatial variability of ecosystem-scale carbon dioxide, water vapor, and
517 energy flux densities, *Bull. Am. Meteorol. Soc.*, 82, 2415–2434, [https://doi.org/10.1175/1520-0477\(2001\)082<2415:FANTTS>2.3.CO;2](https://doi.org/10.1175/1520-0477(2001)082<2415:FANTTS>2.3.CO;2), 2001.
- 518 Balvanera, P., Quijas, S., Karp, D. S., Ash, N., Bennett, E. M., Boumans, R., et al.: Ecosystem services, in: *The GEO*
519 *Handbook on Biodiversity Observation Networks*, edited by: Walters, M. and Scholes, R. J., Springer, 39–78,
520 https://doi.org/10.1007/978-3-319-27288-7_3, 2017.
- 521 Beer, C., Reichstein, M., Tomelleri, E., Ciais, P., Jung, M., Carvalhais, N., et al.: Terrestrial gross carbon dioxide uptake:
522 global distribution and covariation with climate, *Science*, 329, 834–838, <https://doi.org/10.1126/science.1184984>, 2010.
- 523 Blondel, J. and Aronson, J.: *Biology and Wildlife of the Mediterranean Region*, Oxford University Press, Oxford, 328 pp.,
524 1999.
- 525 Bret-Harte, M. S., Mack, M. C., Goldsmith, G. R., Sloan, D. B., DeMarco, J., Shaver, G. R., et al.: Plant functional types do
526

527 not predict biomass responses to removal and fertilization in Alaskan tussock tundra, *J. Ecol.*, 96, 713–726,
528 <https://doi.org/10.1111/j.1365-2745.2008.01378.x>, 2008.

529 Butchart, S. H. M., Walpole, M., Collen, B., van Strien, A., Scharlemann, J. P. W., Almond, R. E. A., et al.: Global
530 biodiversity: indicators of recent declines, *Science*, 328, 1164–1168, <https://doi.org/10.1126/science.1187512>, 2010.

531 Cabello, J., Alcaraz-Segura, D., Reyes, A., Lourenço, P., Requena, J. M., Bonache, J., et al.: System for monitoring
532 ecosystem functioning of Network of National Parks of Spain with remote sensing, *Rev. Teledetección*, 46, 119,
533 <https://doi.org/10.4995/raet.2016.4122>, 2016.

534 Cabello, J., Fernández, N., Alcaraz-Segura, D., Oyonarte, C., Piñeiro, G., Altesor, A., et al.: The ecosystem functioning
535 dimension in conservation: insights from remote sensing, *Biodivers. Conserv.*, 21, 3287–3305,
536 <https://doi.org/10.1007/s10531-012-0370-7>, 2012.

537 Cazorla, B., Cabello, J., Peñas, J., Garcillán, P. P., Reyes, A., and Alcaraz-Segura, D.: Incorporating ecosystem functional
538 diversity into geographic conservation priorities using remotely-sensed Ecosystem Functional Types, *Ecosystems*,
539 <https://doi.org/10.1007/s10021-020-00497-3>, 2020.

540 Cazorla, B., Cabello, J., Reyes, A., Guirado, E., Peñas, J., Pérez-Luque, A. J., and Alcaraz-Segura, D.: A remote-sensing-
541 based dataset to characterize the ecosystem functioning and functional diversity in the Biosphere Reserve of the Sierra
542 Nevada (southeastern Spain), *Earth Syst. Sci. Data*, 15, 1871–1887, <https://doi.org/10.5194/essd-15-1871-2023>, 2023.

543 Cazorla, B., Garcillán, P. P., Cabello, J., Alcaraz-Segura, D., Reyes, A., and Peñas, J.: Patterns of ecosystem functioning as
544 tool for biological regionalization: the case of the mediterranean-desert-tropical transition of Baja California, *Mediterr. Bot.*,
545 42, e68529, <https://doi.org/10.5209/mbot.68529>, 2021.

546 Chu, H., Luo, X., Ouyang, Z., Chan, W. S., Dengel, S., Biraud, S. C., et al.: Representativeness of eddy-covariance flux
547 footprints for areas surrounding AmeriFlux sites, *Agric. For. Meteorol.*, 301, 108350,
548 <https://doi.org/10.1016/j.agrformet.2021.108350>, 2021.

549 Clark, J. S.: Why species tell more about traits than traits about species: predictive analysis, *Ecology*, 97, 1979–1993,
550 <https://doi.org/10.1002/ecy.1453>, 2016.

551 Costanza, R., d'Arge, R., de Groot, R., Farber, S., Grasso, M., Hannon, B., et al.: The value of the world's ecosystem
552 services and natural capital, *Nature*, 387, 253–260, <https://doi.org/10.1038/387253a0>, 1997.

553 Costanza, R., Wilson, M., Troy, A., Voinov, A., Liu, S., and D'Agostino, J.: The value of New Jersey's ecosystem services
554 and natural capital, Institute for Sustainable Solutions, Burlington, VT, 2006.

555 Díaz, S., Purvis, A., Cornelissen, J. H. C., Mace, G. M., Donoghue, M. J., Ewers, R. M., et al.: Functional traits, the
556 phylogeny of function, and ecosystem service vulnerability, *Ecol. Evol.*, 3, 2958–2975, <https://doi.org/10.1002/ece3.601>,
557 2013.

558 Díaz, S., Settele, J., Brondizio, E., Ngo, H., Guèze, M., Agard, J., et al.: Summary for policymakers of the global assessment
559 report on biodiversity and ecosystem services of IPBES, IPBES Secretariat, Bonn, 2020.

560 Domingo-Marimon, C., Jenerowicz-Sanikowska, M., Pesquer, L., Ruciński, M., Krupiński, M., Woźniak, E., et al.:
561 Developing an early warning land degradation indicator based on geostatistical analysis of Ecosystem Functional Types
562 dynamics, *Ecol. Indic.*, 169, 112815, <https://doi.org/10.1016/j.ecolind.2023.112815>, 2024.

563 Epstein, H. E., Burke, I. C., and Mosier, A. R.: Plant effects on spatial and temporal patterns of nitrogen cycling in shortgrass
564 steppe, *Ecosystems*, 1, 374–385, <https://doi.org/10.1007/s100219900030>, 1998.

565 European Environment Agency: Biogeographical regions dataset, [https://www.eea.europa.eu/data-and-](https://www.eea.europa.eu/data-and-maps/data/biogeographical-regions-europe-3)
566 [maps/data/biogeographical-regions-europe-3](https://www.eea.europa.eu/data-and-maps/data/biogeographical-regions-europe-3), 2016.

567 Fernández, N., Paruelo, J. M., and Delibes, M.: Ecosystem functioning of protected and altered Mediterranean environments:
568 a remote sensing classification in Doñana, Spain, *Remote Sens. Environ.*, 114, 211–220,
569 <https://doi.org/10.1016/j.rse.2009.09.009>, 2010.

570 Franz, D., Acosta, M., Altimir, N., Arriga, N., Arrouays, D., Aubinet, M., et al.: Towards long-term standardised carbon and
571 greenhouse gas observations for monitoring Europe’s terrestrial ecosystems: a review, *Int. Agrophys.*, preprint,
572 <https://doi.org/10.2134/agronj2018.02.0114>, 2018.

573 Funk, J. L., Larson, J. E., Ames, G. M., Butterfield, B. J., Cavender-Bares, J., Firn, J., et al.: Revisiting the holy grail: using
574 plant functional traits to understand ecological processes, *Biol. Rev.*, 92, 1156–1173, <https://doi.org/10.1111/brv.12275>,
575 2017.

576 Gomasasca, U., Duveiller, G., Pacheco-Labrador, J., Ceccherini, G., Cescatti, A., Girardello, M., et al.: Satellite remote
577 sensing reveals the footprint of biodiversity on multiple ecosystem functions across the NEON eddy covariance network,
578 *Environ. Res. Ecol.*, 3, 045003, <https://doi.org/10.1088/2752-664X/ad54fb>, 2024.

579 Hellmann, C., Große-Stoltenberg, A., Thiele, J., Oldeland, J., and Werner, C.: Heterogeneous environments shape invader
580 impacts: integrating environmental, structural and functional effects by isoscapes and remote sensing, *Sci. Rep.*, 7, 4118,
581 <https://doi.org/10.1038/s41598-017-04480-w>, 2017.

582 Huang, X., Xiao, J., and Ma, M.: Evaluating the performance of satellite-derived vegetation indices for estimating gross
583 primary productivity using FLUXNET observations across the globe, *Remote Sens.*, 11, 1823,
584 <https://doi.org/10.3390/rs11151823>, 2019.

585 Hurrell, A.: *The Global Environment*, in: *International Relations Theory Today*, Polity Press, Cambridge, UK, 1995.

586 IGBP: The IGBP-DIS global 1 km land cover data set "DISCover": proposal and implementation plans, report of the Land
587 Cover Working Group of IGBP-DIS, IGBP-DIS Office, Toulouse, France, 1992.

588 Ivits, E., Cherlet, M., Mehl, W., and Sommer, S.: Ecosystem functional units characterized by satellite observed phenology
589 and productivity gradients: a case study for Europe, *Ecol. Indic.*, 27, 17–28, <https://doi.org/10.1016/j.ecolind.2012.11.011>,
590 2013.

591 Jax, K.: *Ecosystem Functioning*, Cambridge University Press, Cambridge, UK, 280 pp.,
592 <https://doi.org/10.1017/CBO9780511781216>, 2010.

593 Jetz, W., McGeoch, M. A., Guralnick, R., Ferrier, S., Beck, J., Costello, M. J., et al.: Essential biodiversity variables for

594 mapping and monitoring species populations, *Nat. Ecol. Evol.*, 3, 539–551, <https://doi.org/10.1038/s41559-019-0826-1>,
595 2019.

596 Jobbágy, E. G., Sala, O. E., and Paruelo, J. M.: Patterns and controls of primary production in the Patagonian steppe: a
597 remote sensing approach, *Ecology*, 83, 307–319, [https://doi.org/10.1890/0012-9658\(2002\)083\[0307:PACOPP\]2.0.CO;2](https://doi.org/10.1890/0012-9658(2002)083[0307:PACOPP]2.0.CO;2),
598 2002.

599 Jung, M., Schwalm, C., Migliavacca, M., Walther, S., Camps-Valls, G., Koirala, S., et al.: Scaling carbon fluxes from eddy
600 covariance sites to globe: synthesis and evaluation of the FLUXCOM approach, *Biogeosciences*, 17, 1343–1365,
601 <https://doi.org/10.5194/bg-17-1343-2020>, 2020.

602 Knox, S. H., Jackson, R. B., Poulter, B., McNicol, G., Fluet-Chouinard, E., Zhang, Z., et al.: FLUXNET-CH4 synthesis
603 activity: objectives, observations, and future directions, *Bull. Am. Meteorol. Soc.*, 100, 2607–2632,
604 <https://doi.org/10.1175/BAMS-D-18-0268.1>, 2019.

605 Kostrowicki, J.: Trends in the transformation of European agriculture, in: *Land Use Changes in Europe*, edited by: Brouwer,
606 F. M., Thomas, A. J., and Chadwick, M. J., Springer Netherlands, Dordrecht, 21–47, [https://doi.org/10.1007/978-94-011-](https://doi.org/10.1007/978-94-011-3060-5_3)
607 [3060-5_3](https://doi.org/10.1007/978-94-011-3060-5_3), 1991.

608 Lauenroth, W. K., Dodd, J. L., and Sims, P. L.: The effects of water- and nitrogen-induced stresses on plant community
609 structure in a semiarid grassland, *Oecologia*, 36, 211–222, <https://doi.org/10.1007/BF00349815>, 1978.

610 Lavorel, S. and Garnier, E.: Predicting changes in community composition and ecosystem functioning from plant traits:
611 revisiting the Holy Grail, *Funct. Ecol.*, 16, 545–556, <https://doi.org/10.1046/j.1365-2435.2002.00664.x>, 2002.

612 Lavorel, S., Diaz, S., Cornelissen, J. H. C., Garnier, E., Harrison, S. P., McIntyre, S., et al.: Plant functional types: are we
613 getting any closer to the Holy Grail?, in: *Terrestrial Ecosystems in a Changing World*, edited by: Canadell, J. G., Pataki, D.
614 E., and Pitelka, L. F., Springer, Berlin, Heidelberg, 149–164, https://doi.org/10.1007/978-3-540-32730-1_13, 2007.

615 Lee, S.-J., Berbery, E. H., and Alcaraz-Segura, D.: The impact of ecosystem functional type changes on the La Plata Basin
616 climate, *Adv. Atmos. Sci.*, 30, 1387–1405, <https://doi.org/10.1007/s00376-012-2071-y>, 2013.

617 Lionello, P., Malanotte-Rizzoli, P., Boscolo, R., Alpert, P., Artale, V., Li, L., et al.: The Mediterranean climate: an overview
618 of the main characteristics and issues, in: *Developments in Earth and Environmental Sciences*, vol. 4, edited by: Lionello, P.,
619 Malanotte-Rizzoli, P., and Boscolo, R., Elsevier, Amsterdam, 1–26, [https://doi.org/10.1016/S1571-9197\(06\)80003-0](https://doi.org/10.1016/S1571-9197(06)80003-0), 2006.

620 Liu, L., Smith, J. R., Armstrong, A. H., Alcaraz-Segura, D., Epstein, H. E., Echeverri, A., et al.: Influences of satellite sensor
621 and scale on derivation of ecosystem functional types and diversity, *Remote Sens.*, 15, 5593,
622 <https://doi.org/10.3390/rs15235593>, 2023.

623 Liu, Y., Wu, C., Wang, X., and Zhang, Y.: Contrasting responses of peak vegetation growth to asymmetric warming:
624 evidences from FLUXNET and satellite observations, *Glob. Change Biol.*, 29, 2363–2379,
625 <https://doi.org/10.1111/gcb.16624>, 2023.

626 Lourenço, P., Alcaraz-Segura, D., Reyes-Díez, A., Requena-Mullor, J. M., and Cabello, J.: Trends in vegetation greenness
627 dynamics in protected areas across borders: what are the environmental controls?, *Int. J. Remote Sens.*, 39, 4699–4713,

628 <https://doi.org/10.1080/01431161.2018.1448485>, 2018.

629 Malaterre, C., Dussault, A. C., Rousseau-Mermans, S., Barker, G., Beisner, B. E., Bouchard, F., et al.: Functional diversity:
630 an epistemic roadmap, *BioScience*, 69, 800–811, <https://doi.org/10.1093/biosci/biz086>, 2019.

631 McNaughton, S. J., Oesterheld, M., Frank, D. A., and Williams, K. J.: Ecosystem-level patterns of primary productivity and
632 herbivory in terrestrial habitats, *Nature*, 341, 142–144, <https://doi.org/10.1038/341142a0>, 1989.

633 Midgley, G. F., Bond, W. J., Kapos, V., Ravilious, C., Scharlemann, J. P. W., and Woodward, F. I.: Terrestrial carbon stocks
634 and biodiversity: key knowledge gaps and some policy implications, *Curr. Opin. Environ. Sustain.*, 2, 264–270,
635 <https://doi.org/10.1016/j.cosust.2010.05.003>, 2010.

636 Migliavacca, M., Musavi, T., Mahecha, M. D., Nelson, J. A., Knauer, J., Baldocchi, D. D., et al.: The three major axes of
637 terrestrial ecosystem function, *Nature*, 598, 468–472, <https://doi.org/10.1038/s41586-021-03939-9>, 2021.

638 Mouillot, D., Graham, N. A. J., Villéger, S., Mason, N. W. H., and Bellwood, D. R.: A functional approach reveals
639 community responses to disturbances, *Trends Ecol. Evol.*, 28, 167–175, <https://doi.org/10.1016/j.tree.2012.10.004>, 2013.

640 Mucina, L.: Biome: evolution of a crucial ecological and biogeographical concept, *New Phytol.*, 222, 97–114,
641 <https://doi.org/10.1111/nph.15609>, 2019.

642 Müller, O. V., Berbery, E. H., Alcaraz-Segura, D., and Ek, M. B.: Regional model simulations of the 2008 drought in
643 southern South America using a consistent set of land surface properties, *J. Clim.*, 27, 6754–6778,
644 <https://doi.org/10.1175/JCLI-D-13-00524.1>, 2014.

645 Myers, N., Mittermeier, R. A., Mittermeier, C. G., da Fonseca, G. A. B., and Kent, J.: Biodiversity hotspots for conservation
646 priorities, *Nature*, 403, 853–858, <https://doi.org/10.1038/35002501>, 2000.

647 Nelson, J. A., Walther, S., Gans, F., Kraft, B., Weber, U., Novick, K., et al.: X-BASE: the first terrestrial carbon and water
648 flux products from an extended data-driven scaling framework, *FLUXCOM-X*, *Biogeosciences*, 21, 5079–5115,
649 <https://doi.org/10.5194/bg-21-5079-2024>, 2024.

650 Nicholson, E., Watermeyer, K. E., Rowland, J. A., Sato, C. F., Stevenson, S. L., Andrade, A., et al.: Scientific foundations
651 for an ecosystem goal, milestones and indicators for the post-2020 global biodiversity framework, *Nat. Ecol. Evol.*, 5, 1338–
652 1349, <https://doi.org/10.1038/s41559-021-01538-5>, 2021.

653 Noss, R. F.: Indicators for monitoring biodiversity: a hierarchical approach, *Conserv. Biol.*, 4, 355–364,
654 <https://doi.org/10.1111/j.1523-1739.1990.tb00309.x>, 1990.

655 Noy-Meir, I.: Data transformations in ecological ordination: I. Some advantages of non-centering, *J. Ecol.*, 61, 329–341,
656 <https://doi.org/10.2307/2258933>, 1973.

657 Oki, T., Blyth, E. M., Berbery, E. H., and Alcaraz-Segura, D.: Land use and land cover changes and their impacts on
658 hydroclimate, ecosystems and society, in: *Climate Science for Serving Society: Research, Modeling and Prediction*
659 *Priorities*, edited by: Asrar, G. R. and Hurrell, J. W., Springer Netherlands, Dordrecht, 185–203, https://doi.org/10.1007/978-94-007-6692-1_10, 2013.

660 Pacheco-Labrador, J., Migliavacca, M., Ma, X., Mahecha, M. D., Carvalhais, N., Weber, U., et al.: Challenging the link
661

662 between functional and spectral diversity with radiative transfer modeling and data, *Remote Sens. Environ.*, 280, 113170,
663 <https://doi.org/10.1016/j.rse.2022.113170>, 2022.

664 Palter, J. B.: The role of the Gulf Stream in European climate, *Annu. Rev. Mar. Sci.*, 7, 113–137,
665 <https://doi.org/10.1146/annurev-marine-010814-015656>, 2015.

666 Paruelo, J. M., Jobbágy, E. G., and Sala, O. E.: Current distribution of ecosystem functional types in temperate South
667 America, *Ecosystems*, 4, 683–698, <https://doi.org/10.1007/s10021-001-0148-9>, 2001.

668 Pastorello, G., Trotta, C., Canfora, E., Chu, H., Christianson, D., Cheah, Y. W., et al.: The FLUXNET2015 dataset and the
669 ONEFlux processing pipeline for eddy covariance data, *Sci. Data*, 7, 225, <https://doi.org/10.1038/s41597-020-0534-3>, 2020.

670 Pearson, R. G. and Dawson, T. P.: Predicting the impacts of climate change on the distribution of species: are bioclimate
671 envelope models useful?, *Glob. Ecol. Biogeogr.*, 12, 361–371, <https://doi.org/10.1046/j.1466-822X.2003.00042.x>, 2003.

672 Pereira, H. M., Ferrier, S., Walters, M., Geller, G. N., Jongman, R. H. G., Scholes, R. J., et al.: Essential biodiversity
673 variables, *Science*, 339, 277–278, <https://doi.org/10.1126/science.1229931>, 2013.

674 Pérez-Hoyos, A., Martínez, B., García-Haro, F. J., Moreno, Á., and Gilabert, M. A.: Identification of ecosystem functional
675 types from coarse resolution imagery using a self-organizing map approach: a case study for Spain, *Remote Sens.*, 6, 11391–
676 11419, <https://doi.org/10.3390/rs6111391>, 2014.

677 Petrakis, S., Barba, J., Bond-Lamberty, B., and Vargas, R.: Using greenhouse gas fluxes to define soil functional types, *Plant
678 Soil*, 423, 285–294, <https://doi.org/10.1007/s11104-017-3513-2>, 2018.

679 Pettorelli, N., Bühne, H. S. to, Tulloch, A., Dubois, G., Macinnis-Ng, C., Queirós, A. M., et al.: Satellite remote sensing of
680 ecosystem functions: opportunities, challenges and way forward, *Remote Sens. Ecol. Conserv.*, 4, 71–93,
681 <https://doi.org/10.1002/rse2.59>, 2018.

682 Pettorelli, N., Wegmann, M., Skidmore, A., Múcher, S., Dawson, T. P., Fernandez, M., et al.: Framing the concept of
683 satellite remote sensing essential biodiversity variables: challenges and future directions, *Remote Sens. Ecol. Conserv.*, 2,
684 122–131, <https://doi.org/10.1002/rse2.15>, 2016.

685 Reed, R. A., Peet, R. K., Palmer, M. W., and White, P. S.: Scale dependence of vegetation-environment correlations: a case
686 study of a North Carolina piedmont woodland, *J. Veg. Sci.*, 4, 329–340, <https://doi.org/10.2307/3236104>, 1993.

687 Reichstein, M., Bahn, M., Mahecha, M. D., Kattge, J., and Baldocchi, D. D.: Linking plant and ecosystem functional
688 biogeography, *Proc. Natl. Acad. Sci. USA*, 111, 13697–13702, <https://doi.org/10.1073/pnas.1216065111>, 2014.

689 Requena-Mullor, J. M., López, E., Castro, A. J., Alcaraz-Segura, D., Castro, H., Reyes, A., and Cabello, J.: Remote-sensing
690 based approach to forecast habitat quality under climate change scenarios, *PLoS ONE*, 12, e0172107,
691 <https://doi.org/10.1371/journal.pone.0172107>, 2017.

692 Requena-Mullor, J. M., Quintas-Soriano, C., Brandt, J., Cabello, J., and Castro, A. J.: Modeling how land use legacy affects
693 the provision of ecosystem services in Mediterranean southern Spain, *Environ. Res. Lett.*, 13, 114008,
694 <https://doi.org/10.1088/1748-9326/aae00e>, 2018.

695 Richardson, K., Steffen, W., Lucht, W., Bendtsen, J., Cornell, S. E., Donges, J. F., et al.: Earth beyond six of nine planetary

696 boundaries, *Sci. Adv.*, 9, eadh2458, <https://doi.org/10.1126/sciadv.adh2458>, 2023.

697 Rocchini, D., Bacaro, G., Chirici, G., Da Re, D., Feilhauer, H., Foody, G. M., et al.: Remotely sensed spatial heterogeneity
698 as an exploratory tool for taxonomic and functional diversity study, *Ecol. Indic.*, 85, 983–990,
699 <https://doi.org/10.1016/j.ecolind.2017.11.052>, 2018.

700 Rosenzweig, C. and Dickinson, R. (eds.): *Climate-Vegetation Interactions*, Office for Interdisciplinary Earth Studies,
701 University Corporation for Atmospheric Research, Boulder, CO, USA, 1986.

702 Running, S. W., Baldocchi, D. D., Turner, D. P., Gower, S. T., Bakwin, P. S., and Hibbard, K. A.: A global terrestrial
703 monitoring network integrating tower fluxes, flask sampling, ecosystem modeling and EOS satellite data, *Remote Sens.*
704 *Environ.*, 70, 108–127, [https://doi.org/10.1016/S0034-4257\(99\)00061-9](https://doi.org/10.1016/S0034-4257(99)00061-9), 1999.

705 Running, S. W., Nemani, R. R., Heinsch, F. A., Zhao, M., Reeves, M., and Hashimoto, H.: A continuous satellite-derived
706 measure of global terrestrial primary production, *BioScience*, 54, 547–560, [https://doi.org/10.1641/0006-3568\(2004\)054\[0547:ACSMOG\]2.0.CO;2](https://doi.org/10.1641/0006-3568(2004)054[0547:ACSMOG]2.0.CO;2), 2004.

707
708 Saccone, P., Hoikka, K., and Virtanen, R.: What if plant functional types conceal species-specific responses to environment?
709 Study on arctic shrub communities, *Ecology*, 98, 1600–1612, <https://doi.org/10.1002/ecy.1822>, 2017.

710 Skidmore, A. K., Coops, N. C., Neinavaz, E., Ali, A., Schaepman, M. E., Paganini, M., et al.: Priority list of biodiversity
711 metrics to observe from space, *Nat. Ecol. Evol.*, 5, 896–906, <https://doi.org/10.1038/s41559-021-01451-y>, 2021.

712 Skidmore, A. K., Pettorelli, N., Coops, N. C., Geller, G. N., Hansen, M., Lucas, R., ... & Wegmann, M. Environmental
713 science: Agree on biodiversity metrics to track from space. *Nature*, 523(7561), 403–405. <https://doi.org/10.1038/523403a>,
714 2015.

715 Steffen, W., Richardson, K., Rockström, J., Cornell, S. E., Fetzer, I., Bennett, E. M., et al.: Planetary boundaries: guiding
716 human development on a changing planet, *Science*, 347, 1259855, <https://doi.org/10.1126/science.1259855>, 2015.

717 Suding, K. N. and Goldstein, L. J.: Testing the Holy Grail framework: using functional traits to predict ecosystem change,
718 *New Phytol.*, 180, 559–562, <https://doi.org/10.1111/j.1469-8137.2008.02667.x>, 2008.

719 Sundseth, K.: Natura 2000 in the Alpine region, European Commission, <https://doi.org/10.2779/84763>, 2009a.

720 Sundseth, K.: Natura 2000 in the Continental region, European Commission, <https://doi.org/10.2779/29261>, 2009b.

721 Thomas, H. J. D., Myers-Smith, I. H., Bjorkman, A. D., Elmendorf, S. C., Blok, D., Cornelissen, J. H. C., et al.: Traditional
722 plant functional groups explain variation in economic but not size-related traits across the tundra biome, *Glob. Ecol.*
723 *Biogeogr.*, 28, 78–95, <https://doi.org/10.1111/geb.12856>, 2019.

724 Tilman, D., Isbell, F., and Cowles, J. M.: Biodiversity and ecosystem functioning, *Annu. Rev. Ecol. Evol. Syst.*, 45, 471–
725 493, <https://doi.org/10.1146/annurev-ecolsys-120213-091917>, 2014.

726 Vargas, R., Sonnentag, O., Abramowitz, G., Carrara, A., Chen, J. M., Ciais, P., et al.: Drought influences the accuracy of
727 simulated ecosystem fluxes: a model-data meta-analysis for Mediterranean oak woodlands, *Ecosystems*, 16, 749–764,
728 <https://doi.org/10.1007/s10021-013-9648-1>, 2013.

729 Vaz, A. S., Alcaraz-Segura, D., Campos, J. C., Vicente, J. R., and Honrado, J. P.: Managing plant invasions through the lens

730 of remote sensing: a review of progress and the way forward, *Sci. Total Environ.*, 642, 1328–1339,
731 <https://doi.org/10.1016/j.scitotenv.2018.06.142>, 2018.

732 Villarreal, S., Guevara, M., Alcaraz-Segura, D., and Vargas, R.: Optimizing an environmental observatory network design
733 using publicly available data, *J. Geophys. Res. Biogeosci.*, 124, 1812–1826, <https://doi.org/10.1029/2018JG004776>, 2019.

734 Villarreal, S., Guevara, M., Alcaraz-Segura, D., Brunsell, N. A., Hayes, D., Loescher, H. W., and Vargas, R.: Ecosystem
735 functional diversity and the representativeness of environmental networks across the conterminous United States, *Agric. For.
736 Meteorol.*, 262, 423–433, <https://doi.org/10.1016/j.agrformet.2018.07.026>, 2018.

737 Villarreal, S. and Vargas, R.: Representativeness of FLUXNET sites across Latin America, *J. Geophys. Res. Biogeosci.*,
738 126, e2020JG006090, <https://doi.org/10.1029/2020JG006090>, 2021.

739 Villarreal, S. and Vargas, R.: Representativeness of FLUXNET sites across Latin America, *J. Geophys. Res. Biogeosci.*,
740 126, e2020JG006090, <https://doi.org/10.1029/2020JG006090>, 2021.

741 Violle, C., Reich, P. B., Pacala, S. W., Enquist, B. J., and Kattge, J.: The emergence and promise of functional biogeography,
742 *Proc. Natl. Acad. Sci. USA*, 111, 13690–13696, <https://doi.org/10.1073/pnas.1415442111>, 2014.

743 Violle, C., Thuiller, W., Mouquet, N., Munoz, F., Kraft, N. J. B., Cadotte, M. W., Livingstone, S. W., and Mouillot, D.:
744 Functional rarity: the ecology of outliers, *Trends Ecol. Evol.*, 32, 356–367, <https://doi.org/10.1016/j.tree.2017.02.002>, 2017.

745 Virginia, R. A. and Wall, D. H.: Ecosystem function, principles of, in: *Encyclopedia of Biodiversity*, edited by: Levin, S. A.,
746 Academic Press, San Diego, 345–352, <https://doi.org/10.1016/B978-0-12-384719-5.00031-0>, 2001.

747 Vitousek, P. M.: Beyond global warming: ecology and global change, *Ecology*, 75, 1861–1876,
748 <https://doi.org/10.2307/1941591>, 1994.

749 Wang, L., Zhu, H., Lin, A., Zou, L., Qin, W., and Du, Q.: Evaluation of the latest MODIS GPP products across multiple
750 biomes using global eddy covariance flux data, *Remote Sens.*, 9, 418, <https://doi.org/10.3390/rs9050418>, 2017.

751 Whittaker, R. J., Nogués-Bravo, D., and Araújo, M. B.: Geographical gradients of species richness: a test of the water–
752 energy conjecture of Hawkins et al. (2003) using European data for five taxa, *Glob. Ecol. Biogeogr.*, 16, 76–89,
753 <https://doi.org/10.1111/j.1466-822X.2006.00268.x>, 2007.

754 Williams, B. K.: Discriminant analysis in wildlife research: theory and applications, in: *The Use of Multivariate Statistics in
755 Studies of Wildlife Habitat*, edited by: Capen, D. E., 59–71, General Technical Report RM-87, U.S. Department of
756 Agriculture, Forest Service, 1981.

757 Williams, B. K.: Some observations of the use of discriminant analysis in ecology, *Ecology*, 64, 1283–1291,
758 <https://doi.org/10.2307/1937839>, 1983.

759 Wullschlegel, S. D., Epstein, H. E., Box, E. O., Euskirchen, E. S., Goswami, S., Iversen, C. M., Kattge, J., Norby, R. J., van
760 Bodegom, P. M., and Xu, X.: Plant functional types in Earth system models: past experiences and future directions for
761 application of dynamic vegetation models in high-latitude ecosystems, *Ann. Bot.*, 114, 1–16,
762 <https://doi.org/10.1093/aob/mcu077>, 2014.

763 Xiao, H., McDonald-Madden, E., Sabbadin, R., Peyrard, N., Dee, L. E., and Chadés, I. The value of understanding feedbacks
764 from ecosystem functions to species for managing ecosystems. *Nature Communications*, 10(1),
765 3901. <https://doi.org/10.1038/s41467-019-11890-7>, 2019.

766 Zhang, Y., Song, C., Sun, G., Band, L. E., McNulty, S., Noormets, A., Zhang, Q., and Zhang, Z.: Development of a coupled
767 carbon and water model for estimating global gross primary productivity and evapotranspiration based on eddy flux and
768 remote sensing data, *Agric. For. Meteorol.*, 223, 116–131, <https://doi.org/10.1016/j.agrformet.2016.04.019>, 2016.

769

770 **Biosketch**

771 Beatriz Cazorla is a postdoc whose research focuses on remotely sensed ecosystem functioning at regional scales, their
772 conservation, and their relationship with global change. All other authors are expert in ecosystem functioning, remote sensing,
773 regional ecology, biogeography or energy fluxes.

774

← **Con formato:** Espacio Antes: 12 pto, Después: 12 pto